S Matrix of a Broad Wall Coupler Between Dissimilar Rectangular Waveguides

A. Datta, A. M. Rajeek, A. Chakrabarty, and B. N. Das

***Abstract*—The paper describes a method of moment analysis of a four-port junction between two dissimilar rectangular waveguides coupled through either a longitudinal slot or a transverse slot on the common broad wall. The Green's function approach has been used to obtain the scattered field inside the primary and the secondary waveguide for both cases. The coupled integro-differential equations, arising from the continuity of the tangential component of the magnetic field at both the interfaces of the slot, are transformed into matrix equation using entire domain sinusoidal basis functions in conjunction with global Galerkin's technique. The results obtained using the present method have been compared with the results available in the literature. The theoretical results on the magnitude and phase of the scattering parameters have been compared with the experimental results for the case of a longitudinal slot coupler with moderate offset from the centerline. The use of global sinusoidal basis functions gives a much faster rate of convergence compared to the use of subsectional basis functions. The equivalent loading of a single slot derived in the paper can be effectively utilized to design a multiaperture coupler.**

I. Introduction

THE PARALLEL waveguide couplers are useful for measuring high powers. They can be used in a signal generator for making low-level signal tests on receivers. The parallel couplers may be of two types—broad wall couplers and narrow wall couplers. The broad wall couplers are inherently broader band than the narrow wall couplers, but the latter are useful in high-power applications. The objective of the present work is to study broad wall, long slot coupling, which is likely to lead to a directional coupler with a small number of elements. The analysis of broad wall slot coupling between waveguides of dissimilar broad wall dimensions has gained importance for the purpose of launching power through a standard waveguide and radiating the coupled power from a broad wall slot array cut on a non-standard rectangular waveguide of larger, broader dimension. This is going to help the designer when the slot array is to be designed at a frequency near the cutoff frequency of standard waveguides, where the guide wavelength is unusually high and the characteristic impedance is very sensitive to frequency. So, it is believed worthwhile to present the most generalized and very accurate analysis of a broad wall coupler between waveguides of dissimilar, broader dimensions.

Manuscript received March 2, 1993; revised February 22, 1994.
The authors are with the Department of Electronics and Electrical Communication Engineering, Indian Institute of Technology, Kharagpur-721302, India.
IEEE Log Number 9406814.

The earliest treatment of slots in waveguides are due to Bethe [1] and Stevenson [2]. The theory of Stevenson is basically applicable to narrow resonant slots in thin-walled waveguides. Bethe's theory, on the other hand, was originally developed for very small apertures and was later modified by Cohn [3] for large apertures of finite thickness. The modified Bethe-Cohn theory has been applied to the design of multiaperture couplers by Levy [4]. Among the other methods, a few are the variational technique [5], the method based upon self-reaction [6], and the method of moments [7], [8]. The most recent of these [8] has used a cavity model for the thick slot with rooftop basis functions and has given results for the case of coupling between two identical waveguides. Though the method is quite rigorous, the author has not mentioned anything about the number of rooftop basis functions used in the computation. The case of coupling between two dissimilar waveguides has also not been presented. Moreover, all the results presented in this paper are for amplitude only. It is well known that the phase of the scattering coefficients are very sensitive, and the quality of the numerical solution should be assessed in terms of the discrepancies between the theoretical and experimental values of phase data (in addition to amplitude data). Therefore, no phase information for theory and experiment is presented [8], so, we feel that it is worthwhile to analyze the structure using a much faster numerical technique.

The present paper describes a method of moment analysis of coupling between two dissimilar rectangular waveguides through either a longitudinal slot or transverse slot on the common broad wall. The thick slot has been treated as a stub waveguide [11] and the continuity of the tangential component of the magnetic field has been satisfied at both slot apertures. The integro-differential equations are then solved using global sinusoidal basis functions and Galerkin's technique, where a lesser number of basis functions are required for the convergence of the results compared to the use of subsectional basis functions [7], [8]. Moreover, the Green's function converges for the transverse slot discontinuity without imposition of the so-called "edge condition" [9], [10]. The scattering parameters, and hence, the equivalent network at the plane of symmetry of the slot, have also been determined. The equivalent loading derived in this paper can be effectively utilized to design a multiaperture coupler. The computed results are compared with the results available in the published literature [8] for the limiting case of coupling between two identical waveguides. The theoretical results on the magnitude and phase of the scattering coefficients have also been compared with the

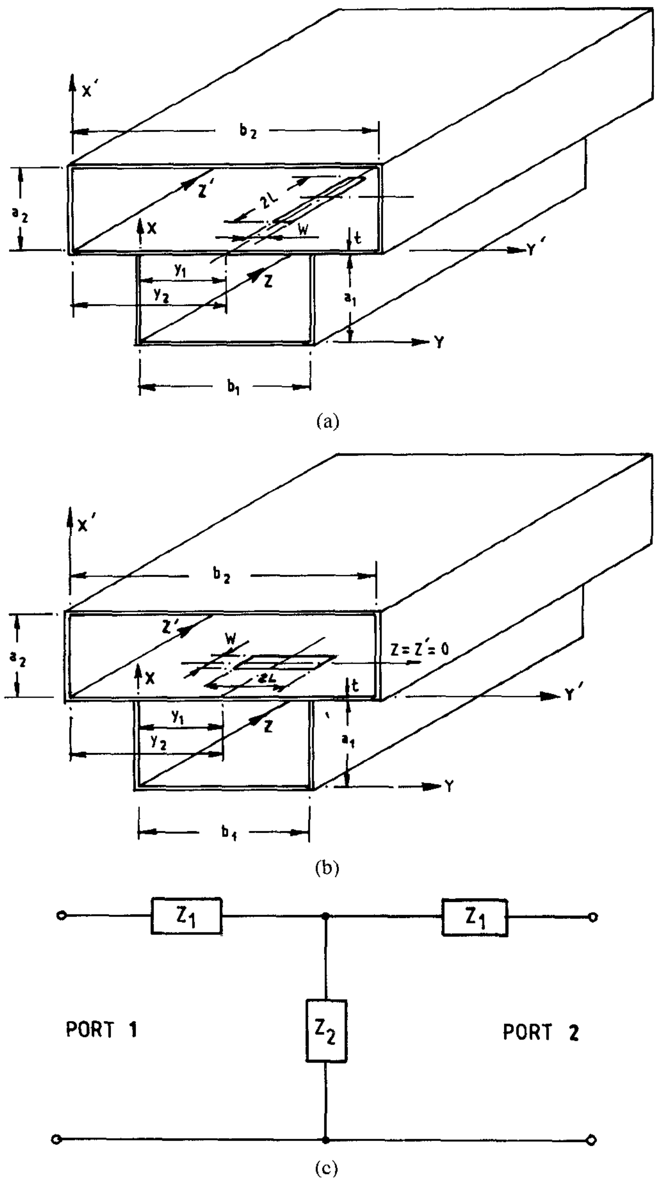

Fig. 1. (a) Two dissimilar rectangular wavelguides coupled through a broad wall longitudinal slot. (b) Two dissimilar rectangular waveguides coupled through a transverse slot at the common broad wall. (c) Equivalent circuit at the plane of symmetry of the slot.

experimental results for the case of longitudinal slot coupling. The agreement between the results obtained using the present method and the experimental results is excellent.

II. Analysis of Longitudinal Slot Coupler

Fig. 1(a) shows two dissimilar rectangular waveguides of cross-sections $a_1 \times b_1$ and $a_2 \times b_2$ coupled through an offset longitudinal slot. For the sake of analysis, the thick slot is treated as a section of a stub waveguide having dimension $2L \times W \times t$. The effect of higher-order modes inside the stub waveguide and multiple reflections from both the interfaces are also considered.

Because of the dominant mode excitation of the primary waveguide, the y-directed electric field at the lower interface is given by

$$\vec{E}_{y1} = \hat{y}\sum_{q=1}^{N}(A_q^+ + A_q^-)e_q^1$$

where

$$e_q^1 = \sin\left\{\frac{q\pi}{2L}(z+L)\right\} \quad \text{for } -L \le z \le L, \quad y_1 - \frac{W}{2} \le y \le y_1 + \frac{W}{2} \quad \text{and} \quad x = a_1 \qquad (1)$$

and at the upper interface is given by

$$\vec{E}_{y2} = \hat{y}\sum_{q=1}^{N}(B_q^+ + B_q^-)e_q^2$$

where

$$e_q^2 = \sin\left\{\frac{q\pi}{2L}(z+L)\right\} \quad \text{for } -L \le z \le L, \quad y_2 - \frac{W}{2} \le y' \le y_2 + \frac{W}{2} \quad \text{and} \quad x' = 0 \qquad (2)$$

This assumption of uniform field along the width of the slot gives a simple, yet accurate, solution for a moderate ratio of slot length to width.

Following the procedure described in Section VII-B of [2], the z-directed magnetic field inside the primary $(H_z^1(e_q^1))$ and the secondary $(H_z^2(e_q^2))$ waveguides due to qth half sinusoidal variation of field in the slot aperture are evaluated. The expression for the magnetic fields inside the primary $(i = 1)$ and the secondary $(i = 2)$ waveguide is given by

$$\begin{aligned} H_z^i(e_q^i) &= \frac{-(-1)^i}{j\omega\mu}\sum_m^{\infty}\sum_n^{\infty}\frac{\epsilon_m\epsilon_n}{a_i b_i}\frac{W\cos(m\pi)\cos\left(\frac{n\pi y_i}{b_i}\right)}{\left[\gamma_{mni}^2 + \left(\frac{q\pi}{2L}\right)^2\right]} \\ &\cdot \operatorname{sinc}\left(\frac{n\pi W}{2b_i}\right)\cos\left(\frac{m\pi x}{a_i}\right)\cos\left(\frac{n\pi y}{b_i}\right) \\ &\cdot \left[\left\{\left\{k^2 - \left(\frac{q\pi}{2L}\right)^2\right\}\right\}\sin\frac{q\pi}{2L}(z+L) + \frac{q\pi}{4L\gamma_{mni}} \right. \\ &\left. \cdot \left[e^{-\gamma_{mni}(z+L)} \pm e^{\gamma_{mni}(z-L)}\right]\{k^2 + \gamma_{mni}^2\}\right] \\ &q \text{ odd/even} \end{aligned} \qquad (3)$$

The expression for γ_{mni} appearing in (3) is given by

$$\gamma_{mni} = \sqrt{\left(\frac{m\pi}{a_i}\right)^2 + \left(\frac{n\pi}{b_i}\right)^2 - k^2} \qquad (4)$$

Satisfying the boundary condition of the tangential component of the magnetic field at lower and upper interfaces, the following set of operator equations is formed.

$$\sum_{q=1}^{N}A_q^+[-Y_q e_q^1 + H_z^1(e_q^1)] + \sum_{q=1}^{N}A_q^-[Y_q e_q^1 + H_z^1(e_q^1)] = -H_z^{inc} \qquad (5)$$

$$\sum_{q=1}^{N} B_q^+[-Y_q e_q^2 + H_z^2(e_q^2)] + \sum_{q=1}^{N} B_q^-[Y_q e_q^2 + H_z^2(e_q^2)] = 0 \quad (6)$$

Taking the scalar product of (5) and (6) with e_p^1 (obtained on replacing q by p in (1)) and e_p^2 (obtained on replacing q by p in (2)) and substituting the relations

$$[B^+] = [\phi][A^+] \quad \text{and} \quad [B^-] = [\phi]^{-1}[A^-] \quad (7)$$

the following set of matrix equations is generated:

$$[M_1^i][A^+] + [M_2^i][A^-] = [G_z^{inc}] \quad (8)$$

$$[M_3^o][A^+] + [M_4^o][A^-] = [0] \quad (9)$$

The matrix $[\phi]$ appearing in (7) is a diagonal matrix whose elements are given by (2.43) of [13].

Y_q is the modal admittance of the TE_{0q} mode inside the stub waveguide the expression for which is given by

$$Y_q = \frac{\gamma_{oq}}{j\omega\mu}; \quad \text{where} \quad \gamma_{oq} = \sqrt{\left(\frac{q\pi}{2L}\right)^2 - k^2} \quad (10)$$

The elements of the square matrices $[M_1^i]$ and $[M_2^i]$ of order N can be computed by the following expressions.

$$(M_1^i)_{pq} = -Y_q\langle e_q^1, e_p^1\rangle + \langle H_z(e_q^1), e_p^1\rangle \quad (11)$$

$$(M_2^i)_{pq} = Y_q\langle e_q^1, e_p^1\rangle + \langle H_z(e_q^1), e_p^1\rangle \quad (12)$$

The square matrices $[M_3^o]$ and $[M_4^o]$ of order N are given by

$$[M_3^o] = [M_1^o][\phi] \quad \text{and} \quad [M_4^o] = [M_2^o][\phi]^{-1}. \quad (13)$$

The elements of the square matrices $[M_1^o]$ and $[M_2^o]$ appearing in (13) can be obtained on replacing $H_z^1(e_q^1)$ by $H_z^2(e_q^2)$, e_p^1 by e_p^2 and e_q^1 by e_q^2 in (11) and (12).

The expressions for the scalar product $\langle H_z^i(e_q^i), e_p^i\rangle$ and $(i = 1, 2)$ can be obtained using expressions (1)–(3).

The elements of the column matrix $[G_z^{inc}]$ can be obtained by using the expression for H_z^{inc} and the expression given by (1).

The expression for γ_{011} can be obtained from (4) by substituting $m = 0$, $n = 1$ and $i = 1$.

From (8) and (9), the coefficients $[A^+]$ and $[A^-]$ and hence, $[B^+]$ and $[B^-]$ are determined. These known values of the coefficients are used in the following expressions to evaluate the dominant mode scattering parameters inside the primary and secondary waveguides.

$$S_{11|z=0} = \sum_{q=1}^{N}(A_q^+ + A_q^-)Q_1\{e^{\gamma_{011}L} \pm e^{-\gamma_{011}L}\}_{q\text{even}}^{q\text{odd}} \quad (14)$$

$$S_{21|z=0} = 1.0 + \sum_{q=1}^{N}(A_q^+ + A_q^-)Q_1\{e^{-\gamma_{011}L} \pm e^{\gamma_{011}L}\}_{q\text{even}}^{q\text{odd}} \quad (15)$$

$$S_{31|z'=0} = \sum_{q=1}^{N}(B_q^+ + B_q^-)Q_2\{e^{\gamma_{012}L} \pm e^{-\gamma_{012}L}\}_{q\text{even}}^{q\text{odd}} \quad (16)$$

$$S_{41|z'=0} = \sum_{q=1}^{N}(B_q^+ + B_q^-)Q_2\{e^{-\gamma_{012}L} \pm e^{\gamma_{012}L}\}_{q\text{even}}^{q\text{odd}} \quad (17)$$

where

$$Q_i = \frac{Wq}{4La_i\gamma_{01i}}\left(\frac{\pi}{b_i}\right)^2 \cos\left(\frac{\pi y_i}{b_i}\right) \cdot \text{sinc}\left(\frac{\pi W}{2b_i}\right) \Big/ \left\{\gamma_{01i}^2 + \left(\frac{q\pi}{2L}\right)^2\right\}$$

In this context, it is worth evaluating the expression for the loading due to the slot as seen at the $z = 0$ plane of the primary waveguide. The expressions for series (Z_1) and shunt (Z_2) arm of the equivalent T-network, as shown in Fig. 1(c), are given by the following expressions:

$$Z_1 = (1 + S_{11|z=0} - S_{21|z=0})/(1 - S_{11|z=0} + S_{21|z=0}) \quad (18)$$

and

$$Z_2 = 2S_{21|z=0}/((1 - S_{11|z=0} + S_{21|z=0}) \cdot (1 - S_{11|z=0} - S_{21|z=0})) \quad (19)$$

III. Analysis of Transverse Slot Coupler

Fig. 1(b) shows two dissimilar rectangular waveguides of cross-sections $a_1 \times b_1$ and $a_2 \times b_2$ coupled through a transverse slot on the broad wall. For the sake of analysis, the coupling slot is assumed as a section of a stub waveguide with dimension $2L \times W \times t$. The effect of higher-order modes inside the stub waveguide and the multiple reflections from both the interfaces are considered.

Because of the dominant mode excitation of the rectangular waveguide, the z-directed electric field at the lower interface is given by

$$\vec{E}_{z1} = \hat{z}\sum_{q=1}^{N}(A_q^+ + A_q^-)e_q^1$$

where

$$e_q^1 = \sin\left\{\frac{q\pi}{2L}(y - y_1 + L)\right\} \quad \text{for} \quad -\frac{W}{2} \le z \le \frac{W}{2}, \quad y_1 - L \le y \le y_1 + L \quad \text{and} \quad x = a_1 \quad (20)$$

and at the upper interface is given by

$$\vec{E}_{z2} = \hat{z}\sum_{q=1}^{N}(B_q^+ + B_q^-)e_q^2$$

where

$$e_q^2 = \sin\left\{\frac{q\pi}{2L}(y' - y_2 + L)\right\} \quad \text{for} \quad -\frac{W}{2} \le z' \le \frac{W}{2}, \quad y_2 - L \le y' \le y_2 + L \quad \text{and} \quad x' = 0 \quad (21)$$

Following the procedure described in Section VII-B of [12], the y-directed magnetic fields inside the primary ($i = 1$) and secondary ($i = 2$) waveguides are evaluated and given below.

$$\begin{aligned} &H_y^i(e_q^i) \\ &= (-1)^i \sum_{m=0}^{\infty}\sum_{n=1}^{\infty} \frac{1}{j\omega\mu} \frac{\epsilon_m}{a_i b_i} \frac{\cos(m\pi)}{\gamma_{mni}^2} \cos\left(\frac{m\pi x}{a_i}\right) \\ &\cdot \sin\left(\frac{n\pi y}{b_i}\right) \frac{\left(\frac{q\pi}{2L}\right)\left(k^2 - \left(\frac{n\pi}{b_i}\right)^2\right)}{\left(\left(\frac{q\pi}{2L}\right)^2 - \left(\frac{n\pi}{b_i}\right)^2\right)} \\ &\cdot \left\{\sin\left[\frac{n\pi}{b_i}(y_i - L)\right] - \cos(q\pi)\sin\left[\frac{n\pi}{b_i}(y_i + L)\right]\right\} \\ &\cdot \left\{2 - e^{-\left(\gamma_{mni}\frac{W}{2}\right)}\left[e^{-\gamma_{mni}z} + e^{\gamma_{mni}z}\right]\right\} \end{aligned} \tag{22}$$

Satisfying the continuity of the y-directed magnetic field at the lower and upper interfaces, the following integro-differential equations are generated:

$$\sum_{q=1}^{N} A_q^+[Y_q e_q^1 + H_y^1(e_q^1)] + \sum_{q=1}^{N} A_q^-[-Y_q e_q^1 + H_y^1(e_q^1)] = -H_y^{inc} \tag{23}$$

$$\sum_{q=1}^{N} B_q^+[Y_q e_q^2 + H_y^2(e_q^2)] + \sum_{q=1}^{N} B_q^-[-Y_q e_q^2 + H_y^2(e_q^2)] = 0 \tag{24}$$

Multiplying (23) and (24) by the same set of weighting functions (e_p^1, e_p^2) as the expansion functions (e_q^1, e_q^2), integrating them over the corresponding apertures and the use of (7) gives the following set of matrix equations.

$$[M_1^i][A^+] + [M_2^i][A^-] = -[G_y^{inc}] \tag{25}$$

$$[M_3^o][A^+] + [M_4^o][A^-] = [0] \tag{26}$$

The elements of the square matrices $[M_1^i]$ and $[M_2^i]$ are of the form,

$$(M_1^i)_{pq} = Y_q\langle e_q^1, e_p^1\rangle + \langle H_y(e_q^1), e_p^1\rangle \tag{27}$$

$$(M_2^i)_{pq} = -Y_q\langle e_q^1, e_p^1\rangle + \langle H_y(e_q^1), e_p^1\rangle \tag{28}$$

The square matrices $[M_3^o]$ and $[M_4^o]$ are given by (13).

Y_q is the modal admittance of the TE_{q0} mode inside the stub waveguide, the expression for which is given by (10).

The elements of the square matrices $[M_1^o]$ and $[M_2^o]$ can be obtained from (27) and (28) on replacing e_p^1 and e_p^2 and $H_y^1(e_q^1)$ by $H_y^2(e_q^2)$.

The expressions for the scalar product $\langle H_y^i(e_q^i), e_p^i\rangle$, and ($i = 1, 2$) can be obtained using (20)–(22).

The elements of the column matrix $[G_y^{inc}]$ can be obtained by using the expression for H_y^{inc} and the expression given by (20).

From (28) and (29), the complex coefficients $[A^+]$, $[A^-]$ and subsequently $[B^+]$ and $[B^-]$ are evaluated. These known complex coefficients are then used in the following equations to compute the dominant mode scattering parameters in the primary and the secondary waveguide.

$$S_{11|z=0} = -\sum_{q=1}^{N}(A_q^+ + A_q^-)P_1 \tag{29}$$

$$S_{21|z=0} = 1 - S_{11|z=0} \tag{30}$$

$$S_{31|z'=0} = \sum_{q=1}^{N}(B_q^+ + B_q^-)P_2 \tag{31}$$

$$S_{41|z'=0} = -S_{31|z'=0} \tag{32}$$

where

$$P_i = \frac{q\pi\left(e^{\gamma_{01i}\frac{W}{2}} - e^{-\gamma_{01i}\frac{W}{2}}\right)}{2La_i b_i \gamma_{01i}\left[\left(\frac{q\pi}{2L}\right)^2 - \left(\frac{\pi}{b_i}\right)^2\right]} \cdot \left[\sin\left\{\frac{\pi}{b_i}(y_i - L)\right\} - \cos(q\pi)\sin\left\{\frac{\pi}{b_i}(y_i + L)\right\}\right]$$

The equivalent loading of the transverse slot is a series element. With $Z_2 = \infty$, the equivalent series impedance as shown in Fig. 1(c) can be obtained from the scattering parameters using the expression given by (18).

Because of the unequal port impedances, the scattering parameters are modified to restore the reciprocity property. The expressions for these modified parameters are given below.

$$\tilde{S}_{11} = S_{11}; \quad \tilde{S}_{21} = S_{21}; \quad \tilde{S}_{31} = rS_{31} \quad \text{and} \quad \tilde{S}_{41} = rS_{41} \tag{33}$$

with

$$r = \sqrt{\frac{a_2 b_2 Z_{1c}}{a_1 b_1 Z_{2c}}}$$

where Z_{1c} and Z_{2c} are the characteristic impedances of TE_{01} modes inside the primary and the secondary waveguides, respectively.

IV. Numerical and Experimental Results

The use of equations (1)–(19) and (33) permits evaluation of the coupling ($|\tilde{S}_{31}|$) for a longitudinal slot coupler having $W = 0.15875$ cm, $y_1 = y_2 = 0.14224$ cm, $a_1 = a_2 = 1.016$ cm, $b_1 = b_2 = 2.286$ cm, and $t = 0$ and 0.158 cm at $f = 9.26$ GHz for $2L$ values ranging between 0.4–4.8 cm. The results converge for $m = 50$ and $n = 50$. The discrepancy between the results obtained using 3 and 5 basis functions is negligible. The results are compared with the curves of Fig. 4 of [8]. The data are presented as curves 1–4 in Fig. 2(a).

The use of equations (20)–(33) permits evaluation of the coupling ($|\tilde{S}_{31}|$) for a transverse slot coupler having $W = 0.15875$ cm, $y_1 = y_2 = 1.143$ cm, $a_1 = a_2 = 1.016$ cm, $b_1 = b_2 = 2.286$ cm and $t = 0$ and 0.158 cm at $f = 9.375$ GHz for $2L$ values ranging between 0.4–2.2 cm. The number of waveguide modes taken in the computation are $m = 50$ and

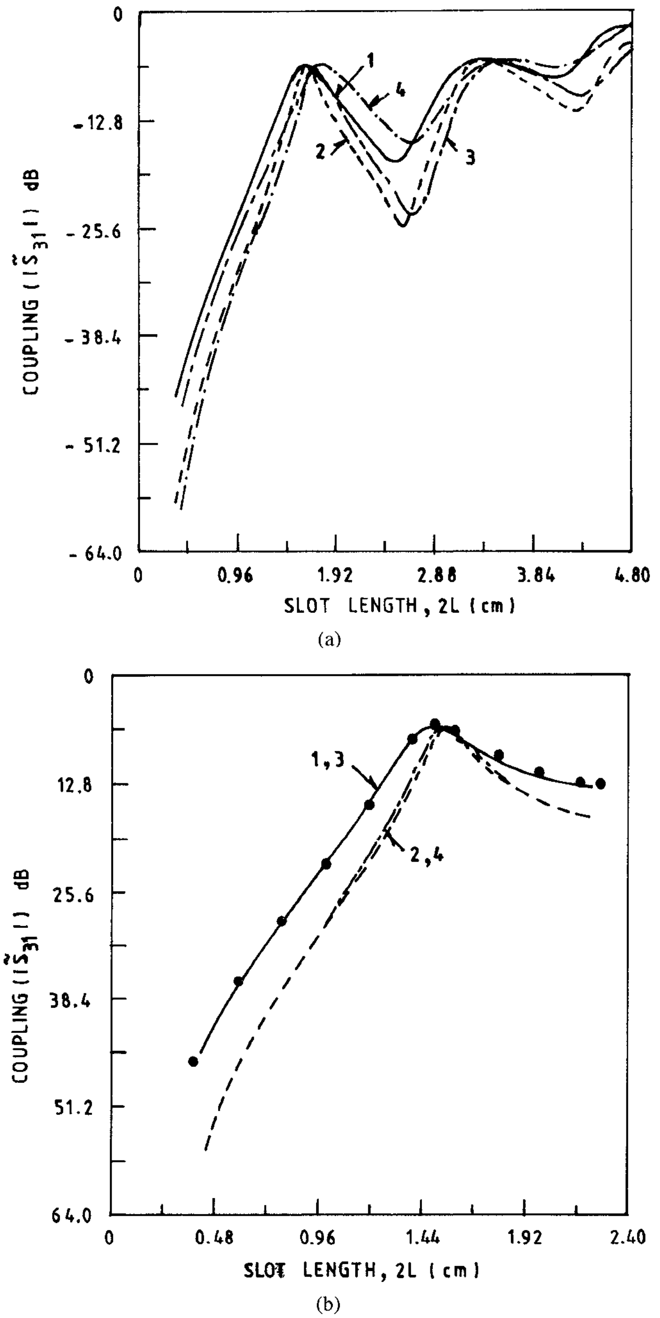

Fig. 2. (a) Variation of the magnitude of $\tilde{S}_{31}$ for a longitudinal slot coupler with slot length. $W = 0.15875$ cm, $y_1 = y_2 = 0.14224$ cm, $a_1 = a_2 = 1.016$ cm, $b_1 = b_2 = 2.286$ cm at $f = 9.26$ GHz. 1) Present method ($t = 0$), 2) Present method ($t = 0.158$ cm), 3) Fig. 4 of [8] ($t = 0$), 4) Fig. 4 of [8] ($t = 0.158$ cm). (b) Variation of the magnitude of $\tilde{S}_{31}$ for a transverse slot coupler with slot length. $W = 0.15875$ cm, $y_1 = y_2 = 1.143$ cm, $a_1 = a_2 = 1.016$ cm, $b_1 = b_2 = 2.286$ cm at $f = 9.375$ GHz. 1) Present method ($t = 0$), 2) Present method ($t = 0.158$ cm), 3) Fig. 3 of [8] ($t = 0$), 4) Fig. 3 of [8] ($t = 0.158$ cm), Variational theory [5].

$n = 50$. The discrepancy between the results obtained using 3 and 5 basis functions is negligible. The results are compared with the curves of Fig. 3 of [8]. The data are presented as curves 1–4 in Fig. 2(b).

With $2L = 1.6$ cm, $W = 0.1$ cm, $a_1 = 1.016$ cm, $b_1 = 2.286$ cm, $y_1 = 0.943$ cm, and $N = 3$ for $t = 0$ and 0.2 cm, the scattering parameters have been computed over a frequency range of 8.0–9.7 GHz for a longitudinal slot

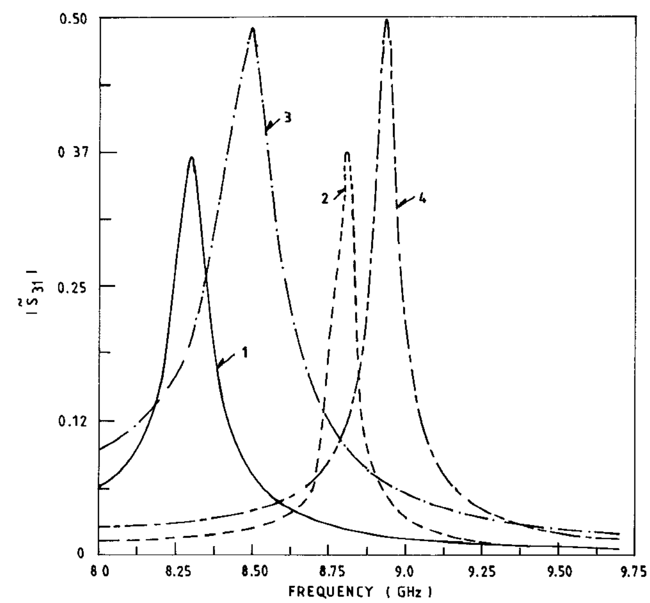

Fig. 3. Variation of the magnitude of coupling coefficient ($\tilde{S}_{31}$) for a longitudinal slot coupler with frequency. $2L = 1.6$ cm, $W = 0.1$ cm, $y_1 = 0.943$ cm, $a_1 = 1.016$ cm, $b_1 = 2.286$ cm. 1) $a_2 = 1.262$ cm, $b_2 = 2.850$ cm, $y_2 = 1.225$ cm, $t = 0$. 2) $a_2 = 1.262$ cm, $b_2 = 2.850$ cm, $y_2 = 1.225$ cm, $t = 0.2$ cm. 3) $a_2 = 1.016$ cm, $b_2 = 2.286$ cm, $y_2 = 0.943$ cm, $t = 0$. 4) $a_2 = 1.016$ cm, $b_2 = 2.286$ cm, $y_2 = 0.943$ cm, $t = 0.2$ cm.

coupler for different sets of secondary waveguide parameters viz. $a_2 = 1.262$ cm, $b_2 = 2.850$ cm, $y_2 = 1.225$ cm and $a_2 = 1.016$ cm, $b_2 = 2.286$ cm, $y_2 = 0.943$ cm.

The computations are repeated for transverse slot coupler for the above four sets of parameters with $y_2 = b_2/2$ and $y_1 = b_1/2$ in all four cases. The results on the magnitude of $\tilde{S}_{31}$ for the four sets of parameters are presented as curves 1–4 in Fig. 3 for the longitudinal slot coupler, and in Fig. 4 for the transverse slot coupler.

The magnitude and phase of coupling coefficient $\tilde{S}_{31}$ has been computed for a longitudinal slot coupler having $2L = 1.56$ cm, $W = 0.1$ cm, $y_1 = y_2 = 0.643$ cm, $a_1 = a_2 = 1.016$ cm, $b_1 = b_2 = 2.286$ cm, and $t = 0.127$ cm over the frequency range of 8.0–11.0 GHz. The other parameters used in the computation are $N = 5$ and $m = n = 50$. The scattering coefficients have also been measured using an HP 8410C Network Analyser setup. The theoretical and experimental data on the magnitude and phase of $\tilde{S}_{31}$ are presented as curves 1 and 2 in Figs. 5 and 6, respectively.

The equivalent T-network of the longitudinal slot coupler, as shown in Fig. 1(c), has been evaluated for $2L = 1.6$ cm, $W = 0.1$ cm, $y_1 = 0.943$ cm, $y_2 = 1.225$ cm, $a_1 = 1.016$ cm, $b_1 = 2.286$ cm, $a_2 = 1.262$ cm, $b_2 = 2.85$ cm, and $t = 0.2$ cm at six different frequencies. The values of the series and shunt arm of the T network are given in Table I.

The equivalent series impedance as shown in Fig. 1(c), ($Z_2 = \infty$), of the transverse slot coupler has been evaluated for $2L = 1.6$ cm, $W = 0.1$ cm, $y_1 = 1.143$ cm, $y_2 = 1.425$ cm, $a_1 = 1.016$ cm, $b_1 = 2.286$ cm, $a_2 = 1.262$ cm, $b_2 = 2.85$ cm, and $t = 0.2$ cm at four different frequencies. The value of the equivalent series impedance has been presented in Table II.

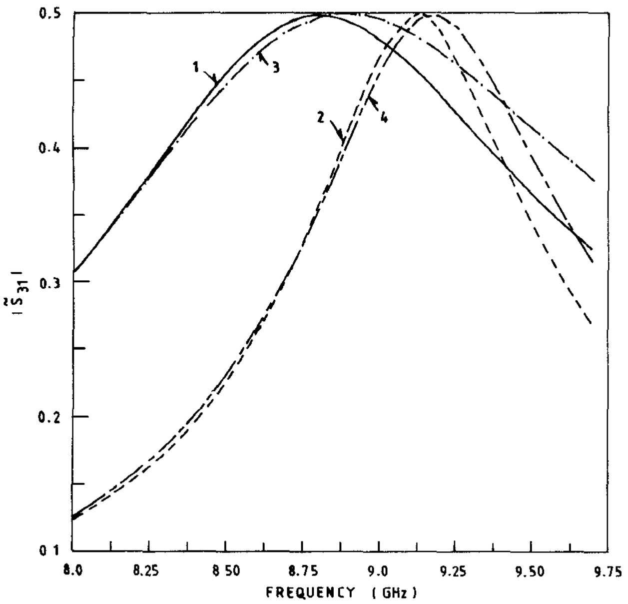

Fig. 4. Variation of the magnitude of coupling coefficient ($\tilde{S}_{31}$) for a transverse slot coupler with frequency. $2L = 1.6$ cm, $W = 0.1$ cm, $y_1 = 1.143$ cm, $a_1 = 1.016$ cm, $b_1 = 2.286$ cm. 1) $a_2 = 1.262$ cm, $b_2 = 2.850$ cm, $y_2 = 1.425$ cm, $t = 0$. 2) $a_2 = 1.262$ cm, $b_2 = 2.850$ cm, $y_2 = 1.425$ cm, $t = 0.2$ cm. 3) $a_2 = 1.016$ cm, $b_2 = 2.286$ cm, $y_2 = 1.143$ cm, $t = 0$. 4) $a_2 = 1.016$ cm, $b_2 = 2.286$ cm, $y_2 = 1.143$ cm, $t = 0.2$ cm.

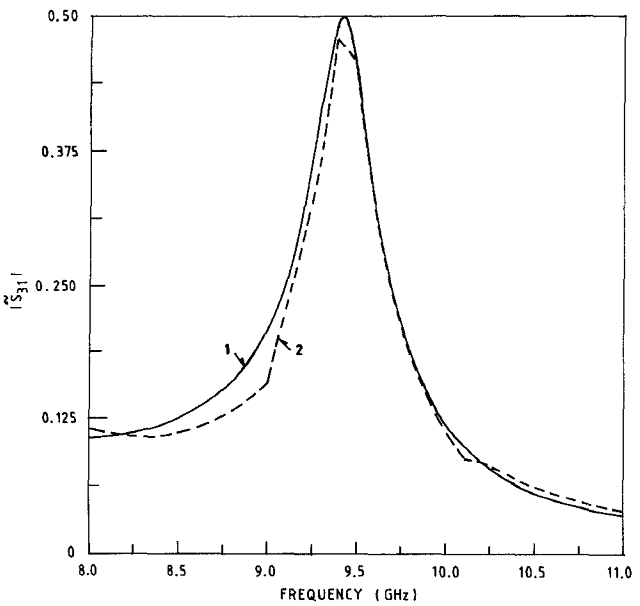

Fig. 5. Variation of the magnitude of coupling coefficient ($\tilde{S}_{31}$) for a longitudinal slot coupler with frequency. $2L = 1.56$ cm, $W = 0.1$ cm, $y_1 = y_2 = 0.643$ cm, $a_1 = a_2 = 1.016$ cm, $b_1 = b_2 = 2.286$ cm, $t = 0.127$ cm. 1) Theoretical curve. 2) Experimental curve.

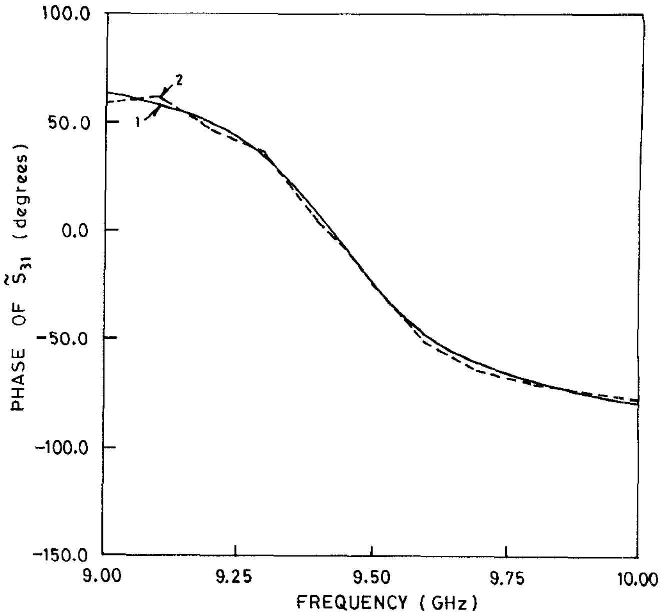

Fig. 6. Variation of the phase of coupling coefficient ($\tilde{S}_{31}$) for a longitudinal slot coupler with frequency. $2L = 1.56$ cm, $W = 0.1$ cm, $y_1 = y_2 = 0.643$ cm, $a_1 = a_2 = 1.016$ cm, $b_1 = b_2 = 2.286$ cm, $t = 0.127$ cm. 1) Theoretical curve. 2) Experimental curve.

TABLE I

Frequency (GHz)	Z_1	Z_2
8.7	j3.91 E-4	0.1020 - j3.6071
8.8	j4.01 E-4	0.1037 - j0.4307
8.81	j4.02 E-4	0.1038 - j0.0952
8.815	j4.03 E-4	0.1039 + j0.0738
8.85	j4.06 E-4	0.1045 + j1.2804
8.9	j4.11 E-4	0.1053 + j3.0768

TABLE II

Frequency (GHz)	$2Z_1$
9.0	0.7419 + j.5863
9.1	1.1823 + j.165
9.2	0.9686 - j.4782
9.3	0.5396 - j.5985

V. Discussion

This paper has described a complete analysis of four-port scattering matrix for a broad wall longitudinal or transverse slot coupler using dissimilar rectangular waveguides. The method of moments has been applied in conjunction with global sinusoidal basis functions and Galerkin's technique to solve the pertinent coupled integro-differential equations.

The results shown in Fig. 2(a) and 2(b) reveal that up to a slot length of 1.5λ, three basis functions are enough to represent the slot aperture field. So, in all further computations of longitudinal and transverse slot coupler, the number of basis functions are taken to be equal to three. The agreement between the results obtained using the present method for a transverse slot coupler and the results given in Fig. 3 of [8] is excellent. However, some discrepancies have been found for longitudinal slot coupler with large offsets and a large length of the slot. For large offsets, the aperture electric field deviates substantially from a half cosinusoid distribution [14]. The inability to capture such a distribution by the sinusoidal global

Galerkin technique may perhaps explain the discrepancy in resonant length computed for $y_1 = y_2 = 0.14224$ cm in Fig. 2(a) of the present work. A piecewise sinusoidal Galerkin or rooftop basis functions [8] would be a better approach for large offsets. But, this would be at the cost of much larger computation time. However, larger offsets are seldom employed in slot couplers or radiators, hence the global Galerkin method is well suited for most applications [14].

Figs. 3 and 4 show that when the primary and the secondary waveguides are non-identical, there is a change in resonance frequency. This frequency also changes with thickness of waveguide wall. The curves for the longitudinal slot coupler (Fig. 3) are very sharp in nature, while those for the transverse slot coupler (Fig. 4) are broader. The bandwidth of the longitudinal slot coupler is, thus, very small.

The agreement between the theoretical and experimental results on the magnitude of coupling coefficient $(\tilde{S}_{31})$ for the case of a longitudinal slot coupler (offset = 5 mm), as shown in Fig. 5, is excellent over a wide band of 3.0 GHz. The agreement between the theoretical and experimental results on the phase of coupling coefficient $(\tilde{S}_{31})$ for the same coupler is excellent over a wide band of 1.0 GHz around the resonant frequency. This excellent agreement justifies the validity of the efficient global Galerkin's technique for the case of a broadwall longitudinal slot coupler.

In order to obtain other scattering parameters, e.g., $\tilde{S}_{13}$, $\tilde{S}_{23}$, and $\tilde{S}_{33}$, etc., the dimensions of the primary and the secondary waveguides only need to be interchanged. The present method of analysis is quite general. The method of analysis presented in Section III can be used in conjunction with the appropriate Green's function for the external region to evaluate the discontinuity offered by a transverse slot radiator. Combination of the two techniques is likely to lead to a simpler convergent solution without the imposition of the edge condition [9].

References

[1] H. A. Bethe, "Theory of diffraction by slots," *Phys. Rev.*, vol. 66, pp. 163–182, 1944.

[2] A. F. Stevenson, "Theory of slots in rectangular waveguides," *J. Appl. Phys.*, vol. 19, pp. 34–38, 1948.

[3] S. B. Cohn, "Microwave coupling by large apertures," *Proc. IRE*, vol. 40, pp. 696–699, 1952.

[4] R. Levy, "Improved single and multiaperture waveguidecoupling theory, including explanation of mutual interaction," *IEEE Trans. Microwave Theory Tech.*, vol. 28, pp. 31–338, 1980.

[5] A. J. Sangster, "Variational method for the analysis of waveguide coupling,"*Proc. IEE*, vol. 112, no. 12, pp. 2171–2179, Dec. 1965.

[6] V. M. Pandharipande and B. N. Das, "Coupling of waveguides through large apertures," *IEEE Trans. Microwave Theory Tech.*, vol. 26, no. 3, pp. 209–212, Mar. 1979.

[7] T. V. Khac, "Studies on slot discontinuities in rectangular waveguide," Ph.D. dissertation, Monash University, Australia, 1974.

[8] S. N. Sinha, "A generalised network formulation for a class of waveguide coupling problems," *IEE Proc.*, Part H, vol. 134, no. 6, pp. 502–508, Dec. 1987.

[9] P. K. Park, G. J. Stern, and R. S. Elliot, "An improved technique for the evaluation of transverse slot discontinuities in rectangular waveguide," *IEEE Trans. Antenn. Propagat*, vol. 31, no. 1, pp. 148–153, Jan. 1983.

[10] J. Meixner, "The behaviour of electromagnetic fields at edges," *IEEE Trans. Antenn. Propagat*, vol. 20, no. 4, pp. 442–446, July 1972.

[11] L. G. Joseffson, "Analysis of longitudinal slots in rectangular waveguides," *IEEE Trans. Antenn. Propagat.*, vol. 35, pp. 1351–1357, 1987.

[12] G. Markov, *Antennas.* Moscow: Progress Publishers, 1965.

[13] P. V. D. S. Rao, "Investigations on slot coupled junctions between rectangular and circular waveguides," Ph.D. dissertation, IIT Kharagpur, India, 1989.

[14] S. R. Rengarajan, "Characteristics of a longitudinal/transverse coupling slot in crossed rectangular waveguides," *IEEE Trans. Microwave Theory Tech.*, vol. 37, no. 8, pp. 1171–1177, Aug. 1989.

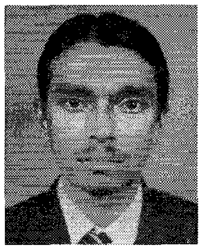

Amlan Datta was born in Calcutta, India, on November 26, 1965. He received the B.Tech., M.Tech., and Ph.D. degrees from Indian Institute of Technology, Kharagpur, India in 1987, 1988, and 1993, respectively. His fields of interest include electromagnetics, microwave circuits, antennas, mathematical techniques used in electromagnetics, and numerical modelling using method of moments.

Currently, he is working as a Project Officer at IIT, Kharagpur.

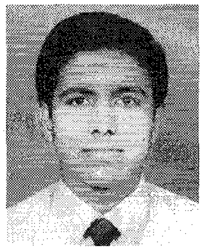

A. Mohammed Rajeek was born in Tirunelveli district, TamilNadu, India on May 25, 1971. He received the B.E. degree in electronics and communication engineering. from College of Engineering., Guindy, Anna University, Madras, India in 1992. He completed his M.Tech. degree in microwave eng. at Indian Institute of Technology, Kharagpur, in 1993, where he is presently a research scholar. His fields of interest include waveguide slot couplers and antennas and numerical methods as applied to electromagnetics.

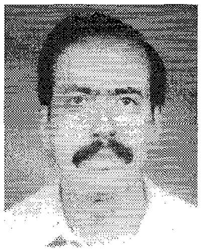

Ajay Chakrabarty received the B.Tech., M. Tech., and Ph.D. degrees from the Indian Institute of Technology, Kharagpur, India in 1975, 1977, and 1982, respectively.

He joined the faculty of the E&ECE Department at IIT Kharagpur in 1980. He worked as a visiting Assistant Professor at Syracuse University from August 1989 to May 1990. His current research interests are antenna pattern synthesis, slot arrays, feed network for phased arrays, and ESD studies. Currently, he is a professor in the E&ECE Department at IIT Kharagpur.

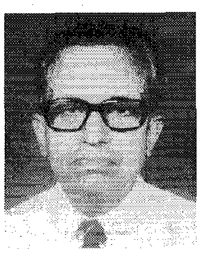

B. N. Das received the Ph.D. degree in electronics and electrical communication engineering from the IIT Kharagpur, in 1967.

From 1958 to 1991, he was in the faculty of the Department of E&ECE at IIT, Kharagpur. He has been actively guiding research in the fields of electromagnetics, microwave networks, antenna pattern synthesis, printed-circuit antennas, slot arrays, phased arrays, striplines, microstriplines, and EMI/EMC studies. He has published more than 100 research papers in journals of the U.S., U.K., U.S.S.R., and India.

Dr. Das is a Fellow of the Indian National Science Academy. At present, he is associated with Department of E&ECE at IIT Kharagpur as an Emeritus Scientist & Emeritus Professor.